The neutrinoless $\beta\beta$ process at the LHC [1]

#Pheno21, University of Pittsburgh

Richard Ruiz

Institute of Nuclear Physics – Polish Academy of Science (IFJ PAN)

25 May 2021

[1] w/ B. Fuks, J. Neundorf, K. Peters, M. Saimpert [2011.02547; 2012.09882]

a fun idea: is it possible to see the (standard mechanism for) neutrinoless $\beta\beta$ process ($0\nu\beta\beta$) at accelerators?

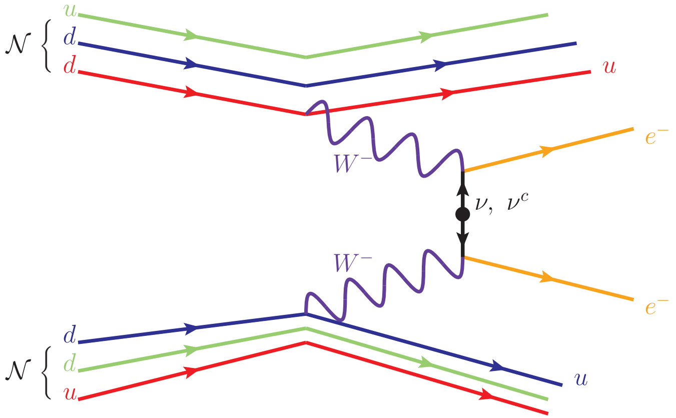

Why? Colliders, beam dumps, etc., can access μ and τ sectors!

for reviews on LNV/LFV at colliders, see w/ Y. Cai, T. Li, T. Han [1711.02180], and w/ S. Pascoli, et. al. [1812.08750]

Many ways to explain $m_\nu \neq 0$, so take an effective field theory approach:

The **Weinberg operator** is the only SMEFT operator at $d = 5$: Weinberg ('97)

$$\mathcal{L} = \frac{C_5^{\ell\ell'}}{\Lambda}[\Phi \cdot \overline{L}_\ell^c][L_{\ell'} \cdot \Phi]$$

Can be generated in **many** ways at tree- and loop-level

Eg. Ma ('98), Bonnet, et al [1204.5862]

Importantly, after EWSB, generates a Majorana mass matrix for ν

$$m_{\ell\ell'} = C_5^{\ell\ell'} \langle \Phi \rangle^2 / 2\Lambda \quad \leftarrow\text{(flavor basis!)}$$

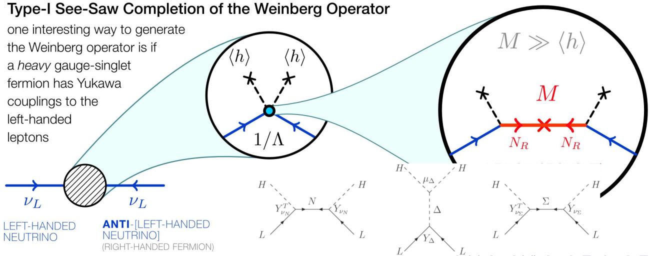

F. Tanedo

constraints on the Weinberg operator from nuclear $0\nu\beta\beta$ decay

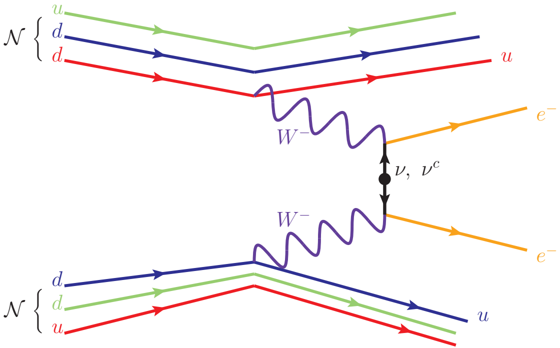

The Weinberg operator:

$$\mathcal{L} = \frac{C_5^{\ell\ell'}}{\Lambda}[\Phi \cdot \overline{L}_\ell^c][L_{\ell'} \cdot \Phi]$$

generates ν mass matrix:

$$m_{\ell\ell'} = C_5^{\ell\ell'} \langle \Phi \rangle^2 / 2\Lambda$$

since

$$|m_{ee}| = \left| \sum_{k=1}^{3} U_{ek} m_{\nu_k} U_{ek} \right|$$

"mass" in flavor space

$\implies$ nuclear $0\nu\beta\beta$ decay rate:

$$1/T_{1/2}^{0\nu\beta\beta} \sim |\mathcal{M}^{0\nu\beta\beta}|^2 \sim |m_{ee}|^2$$

The Weinberg operator:

$$\mathcal{L} = \frac{C_5^{\ell\ell'}}{\Lambda}[\Phi \cdot \overline{L}_\ell^c][L_{\ell'} \cdot \Phi]$$

generates ν mass matrix:

$$m_{\ell\ell'} = C_5^{\ell\ell'} \langle \Phi \rangle^2 / 2\Lambda$$

since

$$|m_{ee}| = \left| \sum_{k=1}^3 U_{ek} m_{\nu_k} U_{ek} \right|$$

"mass" in flavor space

$\Longrightarrow$ nuclear $0\nu\beta\beta$ decay rate:

$$1/T_{1/2}^{0\nu\beta\beta} \sim |\mathcal{M}^{0\nu\beta\beta}|^2 \sim |m_{ee}|^2$$

Plotted: Excluded/allowed "effective $\beta\beta$ Majorana mass" vs lightes m_ν

(assumes no other new physics)

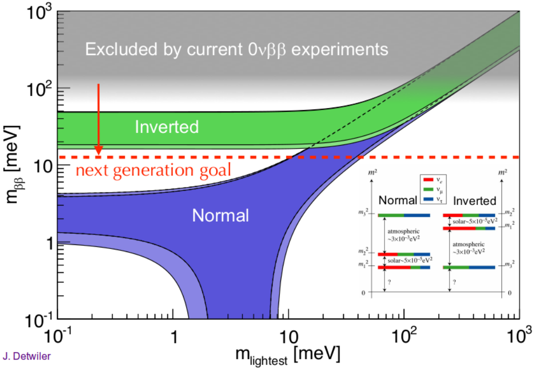

Searches for nuclear $0\nu\beta\beta$ set strong constraints, e.g., GERDA [2009.06079]

$$\Lambda / C_5^{ee} \gtrsim (3.3 - 7.6) \times 10^{14} \text{ GeV}$$

C_5^{ee} **can naturally be zero/small** Eg. symmetry [0810.1263] or interference [Asaka('20)x3]

So what about the other $C_5^{\ell\ell'}$?

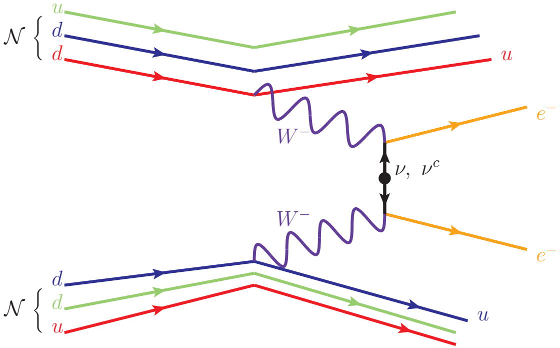

$W^\pm W^\pm$ scattering at dimension five

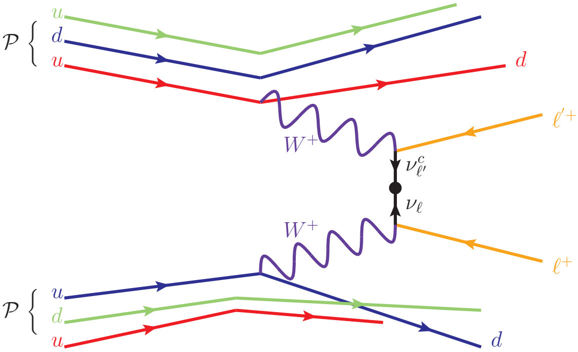

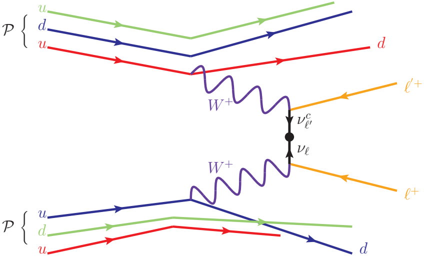

The helicity amplitude for the $0\nu\beta\beta$ process $q\overline{q'} \to \ell_1^+ \ell_2^+ \overline{f} f'$ is

$$\mathcal{M}_{LNV} = J^{\mu}_{f_1 f_1'} J^{\nu}_{f_2 f_2'} \Delta^{W}_{\mu\alpha} \Delta^{W}_{\nu\beta} \underbrace{T^{\alpha\beta}_{LNV} \mathcal{D}(p_\nu)}_{\text{lepton current}}$$

Difficult to simulate events since Weinberg op. modifies propagator of ν_ℓ

modern Monte Carlo tools work in mass basis and do not like the idea of modifying $\langle 0 | \overline{\nu_{\ell'}} \nu_\ell | 0 \rangle$

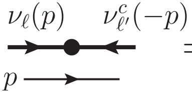

$$= \frac{i\not{p}}{p^2} \frac{-iC_5^{\ell\ell'} v^2}{\Lambda} \frac{i\not{p}}{p^2} = \frac{i m_{\ell\ell'}}{p^2}$$

Solution: Treat vertex as a particle! Invent unphysical Majorana fermion with (small) mass $m_{\ell\ell}$ that couples to all lepton flavors

recovers right behavior!

$$T^{\alpha\beta}_{LNV} \mathcal{D}(p_\nu) \propto \gamma^\alpha P_L \frac{i(\not{p} + m_{\ell\ell'})}{p^2 - m^2_{\ell\ell'}} \gamma^\beta P_R = \gamma^\alpha P_L \frac{i m_{\ell\ell'}}{p^2} P_L \gamma^\beta \times \left[1 + \mathcal{O}\left(\left| \frac{m^2_{\ell\ell'}}{p^2} \right| \right) \right]$$

Plotted: Normalized production rate ($C_5 = 1$) vs scale (Λ)

w/ Fuks, Neundorf, Peters, Saimpert [2012.09882]

Full $2 \to 4$ calculation at NLO(+PS) in QCD is more involved

Used mg5amc + NEW SMWeinberg UFO libraries

Driven by $W_0^+ W_0^+$ scattering

$\hat{\sigma}(W^+W^+ \to \ell^+\ell^+) \sim \frac{|C_5^{\ell\ell}|^2}{18\pi\Lambda^2}$

Once σ is obtained for a "high" scale, i.e., $C_5^{\ell\ell'} = 1, \Lambda = 200$ TeV, rescale for other Λ / C_5.

C_5^{ee}/Λ is heavily constrained. **What can the LHC say about $C_5^{\ell\ell'}$?**

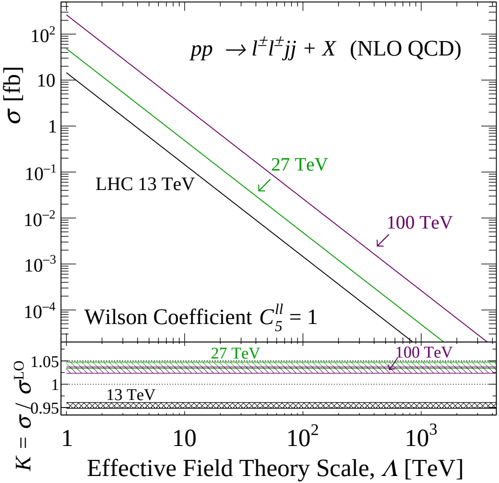

The collider signature exhibits both LNV and VBS characteristics

$$pp \to \mu^\pm \mu^\pm jj + X$$

(L) $E_T^{\rm miss}$ (R) $H_T / p_T^{\mu_1}$

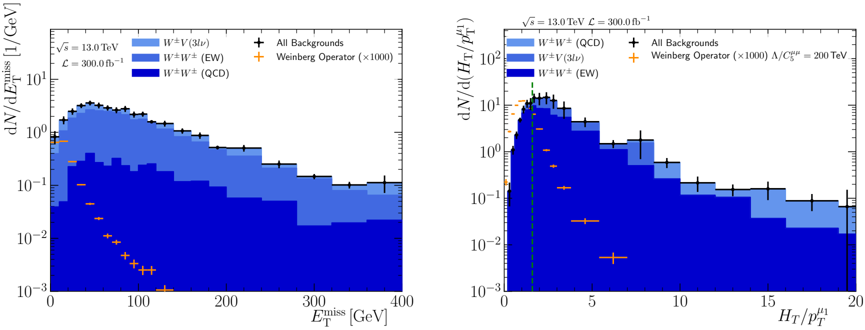

The collider signature exhibits both LNV and VBS characteristics

$$pp \to \mu^{\pm}\mu^{\pm}jj + X$$

- same-sign, high-p_T charged leptons without MET and back-to-back
- forward, high-p_T with rapidity gap
- See backup slides for kinematic distributions at NLO+PS

Built simplified analysis for expedience:

TABLE II. Particle identification and signal region definitions

Particle Identification Cuts
$p_T^{e\ (\mu)\ [j]} > 10\ (10)\ [25]$ GeV, Anti-$k_T(R{=}0.4)$
$\lvert\eta^{e\ (\mu)\ [j]}\rvert < 2.5\ (2.7)\ [4.5]$
Signal Region Cuts
$p_T^{\mu_1\ (\mu_2)} > 27\ (10)$ GeV, $n_\mu = 2$, $n_j \geq 2$,
$n_e = n_{\tau\text{had}} = 0$, $Q_{\mu_1} \times Q_{\mu_2} = 1$, $M(j_1, j_2) > 700$ GeV
$E_T^{\text{miss}} < 30$ GeV, $(H_T/p_T^{\mu_1}) < 1.6$

TABLE III. Expected number of background and $0\nu\beta\beta$ signa events in the signal region with $\mathcal{L} = 300\ \text{fb}^{-1}$ (3 ab^{-1}).

Collider	QCD $W^\pm W^\pm jj$	EW $W^\pm W^\pm jj$	$W^\pm V$	Total	Signal
LHC	< 0.01	6.40	1.16	7.56	0.013
HL-LHC	< 0.01	64.0	11.6	75.5	0.13

the big picture

With a minimal cuts (= can be improved) $\mathcal{L} = 300\ (3000)\ \text{fb}^{-1}$

$$\Lambda/|C_5^{\mu\mu}| \lesssim 8.3\ (11)\ \text{TeV} \implies |m_{\mu\mu}| \gtrsim 7.3\ (5.4)\ \text{GeV}$$

Plotted: Allowed and projected reach of $|m_{\mu\mu}|$ vs lights ν mass

$$|m_{\ell\ell'}| = |C_5^{\ell\ell'}|\langle\Phi\rangle^2/2\Lambda = |\sum_{k=1}^{3} U_{\ell k} m_{\nu_k} U_{\ell' k}|$$

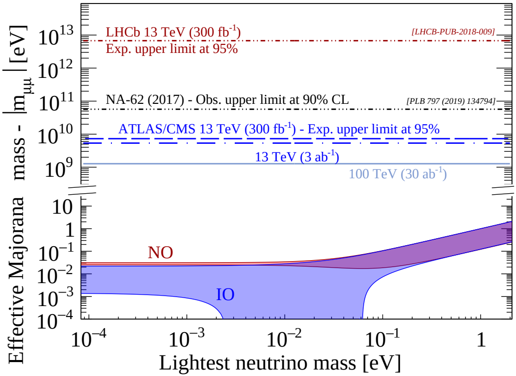

LHC is most competative but all can be improved!

Summary

- Colliders are **incredibly complementary** to oscillation facilities:
  - Direct production of Seesaw and heavy flavors particles
  - Test both neutrino NSIs and UV realizations of EFTs

- If BSM is heavy, the Weinberg op. parametrizes the origin of m_ν
  - $0\nu\beta\beta$ experiments *strongly constrain* Λ/C_5^{ee} but insensitive to μ, τ
  - For high-energy scattering and decay processes, a prescription for describing the Weinberg op. has been developed (and implemented into a UFO!)

    w/ B. Fuks, J. Neundorf, K. Peters, M. Saimpert [2012.09882]

  - For first time, there is a roadmap for probing Weinberg op. with μ, τ at accelerators (LHC, HL-LHC, beam dumps, etc.)

- Lots not covered, so see papers for details! [2011.02547; 2012.09882]

Thank you.

Backup

anatomy of the $0\nu\beta\beta$ process

helicity preservation in $W^-W^+ \to \ell_i^-\ell_j^+$

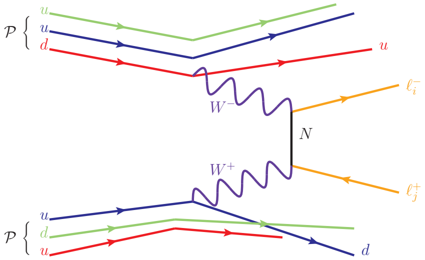

The helicity amplitude for the LNC process $q_1 q_2 \to \ell_1^- \ell_2^+ q_1' q_2'$ is

$$\mathcal{M}_{LNC} = J^{\mu}_{q_1 q_1'} J^{\nu}_{q_2 q_2'} \Delta^W_{\mu\rho} \Delta^W_{\nu\sigma} T^{\rho\sigma}_{LNC} \mathcal{D}(p_N)$$

helicity preservation in $W^- W^+ \to \ell_i^- \ell_j^+$

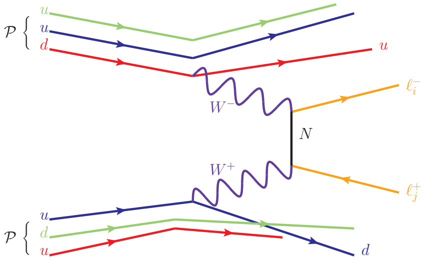

The helicity amplitude for the LNC process $q_1 q_2 \to \ell_1^- \ell_2^+ q_1' q_2'$ is

$$\mathcal{M}_{LNC} = J^{\mu}_{q_1 q_1'} J^{\nu}_{q_2 q_2'} \Delta^W_{\mu\rho} \Delta^W_{\nu\sigma} T^{\rho\sigma}_{LNC} \mathcal{D}(p_N)$$

$$T^{\rho\sigma}_{LNC} = \overline{u_L}(p_1)\gamma^\rho P_L \times (\underbrace{\not{p}_N}_{\text{LH helicity state}} + \underbrace{m_N}_{P_L m_N P_R = 0}) \times \gamma^\sigma P_L v_R(p_2)$$

helicity preservation in $W^-W^+ \to \ell_i^-\ell_j^+$

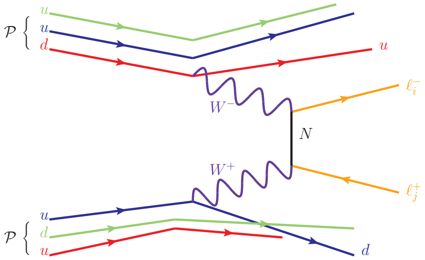

The helicity amplitude for the LNC process $q_1 q_2 \to \ell_1^- \ell_2^+ q_1' q_2'$ is

$$\mathcal{M}_{LNC} = J^{\mu}_{q_1 q_1'} J^{\nu}_{q_2 q_2'} \Delta^W_{\mu\rho} \Delta^W_{\nu\sigma} T^{\rho\sigma}_{LNC} \mathcal{D}(p_N)$$

$$T^{\rho\sigma}_{LNC} = \overline{u_L}(p_1)\gamma^\rho P_L \times (\underbrace{\not{p}_N}_{\text{LH helicity state}} + \underbrace{m_N}_{P_L m_N P_R = 0}) \times \gamma^\sigma P_L v_R(p_2)$$

$$\implies \mathcal{M}_{LNC} \sim \frac{p_N}{(p_N^2 - m_N^2)}$$

scales with momentum-transfer!

helicity inversion in $W^+W^+ \to \ell_i^+\ell_j^+$

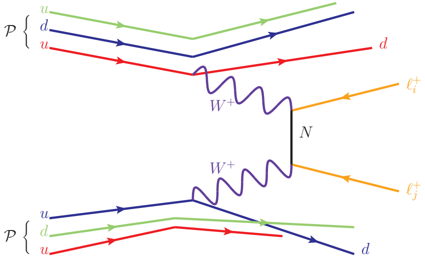

The helicity amplitude for the LNV process $q_1 q_2 \to \ell_1^+ \ell_2^+ q_1' q_2'$ is

$$\mathcal{M}_{LNV} = J^{\mu}_{q_1 q_1'} J^{\nu}_{q_2 q_2'} \Delta^{W}_{\mu\rho} \Delta^{W}_{\nu\sigma} T^{\rho\sigma}_{LNV} \mathcal{D}(p_N)$$

helicity inversion in $W^+W^+ \to \ell_i^+\ell_j^+$

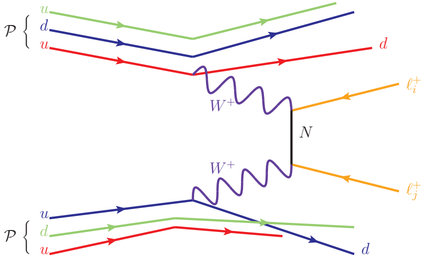

The helicity amplitude for the LNV process $q_1 q_2 \to \ell_1^+\ell_2^+ q_1' q_2'$ is

$$\mathcal{M}_{LNV} = J^{\mu}_{q_1 q_1'} J^{\nu}_{q_2 q_2'} \Delta^{W}_{\mu\rho}\Delta^{W}_{\nu\sigma} T^{\rho\sigma}_{LNV}\mathcal{D}(p_N)$$

Intuition: CPT Theorem $\implies$ CT-inversion = P-inversion

$$T^{\rho\sigma}_{LNV} = \overline{u_R}(p_1)\gamma^{\rho} \underbrace{P_R}_{CPT:\ P_L\to P_R} \times (\underbrace{\not{p}_N}_{P_R\ \not{p}_N\ P_R=0} + \underbrace{m_N}_{\text{RH helicity state}}) \times \gamma^{\sigma} P_L v_R(p_2)$$

helicity inversion in $W^+W^+ \to \ell_i^+\ell_j^+$

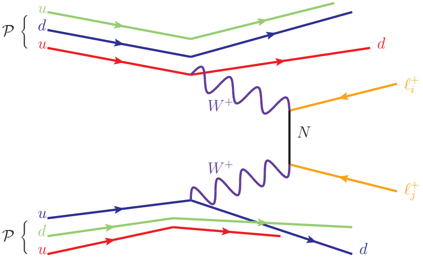

The helicity amplitude for the LNV process $q_1 q_2 \to \ell_1^+\ell_2^+ q_1' q_2'$ is

$$\mathcal{M}_{LNV} = J^{\mu}_{q_1 q_1'} J^{\nu}_{q_2 q_2'} \Delta^W_{\mu\rho}\Delta^W_{\nu\sigma} T^{\rho\sigma}_{LNV}\mathcal{D}(p_N)$$

Intuition: CPT Theorem $\implies$ CT-inversion = P-inversion

$$T^{\rho\sigma}_{LNV} = \overline{u_R}(p_1)\gamma^\rho \underbrace{P_R}_{CPT:\ P_L \to P_R} \times (\underbrace{\not{p}_N}_{P_R\ \not{p}_N\ P_R = 0} + \underbrace{m_N}_{\text{RH helicity state}}) \times \gamma^\sigma P_L v_R(p_2)$$

$$\implies \mathcal{M}_{LNV} \sim \frac{m_N}{(p_N^2 - m_N^2)}$$ scales with mass!

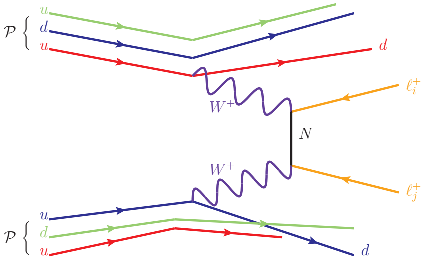

The remainder of $\mathcal{M}_{LNV}$ depends on:
- *WW* scattering system
- *N*'s pole structure

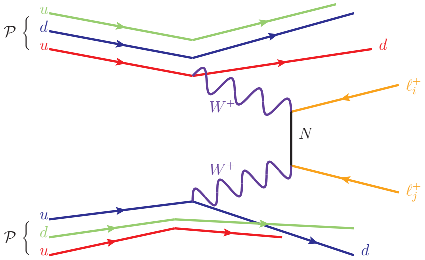

The remainder of $\mathcal{M}_{LNV}$ depends on:

- WW scattering system
- N's pole structure

Explicit computation shows amplitude is driven by $W_0^\pm W_0^\pm$ scattering

$$\mathcal{M}_{LNV} \sim \varepsilon_\mu^{W_1}(\lambda_1)\varepsilon_\mu^{W_2}(\lambda_2) \sim \frac{M_{WW}^2}{M_W^2}$$

"Low-mass" limit ($M_{WW} \gg m_N$):

$$\frac{m_N}{(p_N^2 - m_N^2)} \sim \frac{m_N}{(M_{WW}^2 - m_N^2)} \sim \frac{m_N}{M_{WW}^2} + \mathcal{O}\left(\frac{m_N^2}{M_{WW}^2}, \frac{M_W^2}{M_{WW}^2},\right)$$

(amplitude grows with mass!)

"High-mass" limit ($M_{WW} \ll m_N$):

$$\frac{m_N}{(p_N^2 - m_N^2)} \sim \frac{m_N}{(M_{WW}^2 - m_N^2)} \sim \frac{-m_N}{m_N^2} + \mathcal{O}\left(\frac{M_{WW}^2}{m_N^2}\right)$$

(slower decoupling since $d = 7$, not $d = 8$)

Plotted: Normalized production rate $(\sigma/|V|^{2\ (4)})$ vs mass (m_N)

w/ Fuks, Neundorf, Peters, Saimpert [2011.02547]

Full $2 \to 4$ calculation at NLO (+PS) in QCD is more involved

Used mg5amc + HeavyN UFO libraries

"Low-mass" limit $(M_{WW} \gg m_N)$:

$$\hat{\sigma}(W^+W^+ \to \ell^+\ell^+) \sim g_W^4 |V_{\ell N}|^4 \frac{m_N^2}{m_W^4}$$

"High-mass" limit $(M_{WW} \ll m_N)$:

$$\hat{\sigma}(W^+W^+ \to \ell^+\ell^+) \sim g_W^4 \frac{|V_{\ell N}|^4}{m_N^2} \frac{M_{WW}^4}{m_W^4}$$

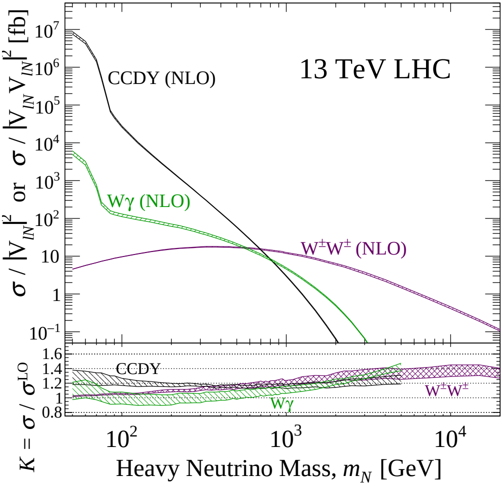

The collider signature exhibits both LNV and VBS/F characteristics

$$pp \to \mu^\pm \mu^\pm jj + X$$

- same-sign, high-p_T charged leptons without MET and back-to-back
- forward, high-p_T with rapidity gap
- See next few slides for kinematic distributions at NLO+PS

Built simplified analysis for expedience:

TABLE III. Pre-selection and signal region cuts.

Pre-selection Cuts
$p_T^{\mu_1\ (\mu_2)} > 27\ (10)$ GeV, $\lvert\eta^\mu\rvert < 2.7$, $n_\mu = 2$,
$p_T^j > 25$ GeV, $\lvert\eta^j\rvert < 4.5$, $n_j \geq 2$,
$Q_{\mu_1} \times Q_{\mu_2} = 1$, $M(j_1, j_2) > 700$ GeV
Signal Region Cuts
$p_T^{\mu_1}$, $p_T^{\mu_2} > 300$ GeV

TABLE I. Generator-level cross sections [fb] and cuts, μ_f, μ_r scale uncertainty [%], PDF uncertainties [%], and perturbative order for leading backgrounds at $\sqrt{s} = 13$ TeV.

Process	Order	Cuts	$\sigma^{\text{Gen.}}$ [fb]	$\pm\delta_{\mu_f,\mu_r}$	$\pm\delta_{\text{PDF}}$
$W^\pm W^\pm jj$ (QCD)	NLO in QCD	Eq. (4.2)	385	$^{+10\%}_{-10\%}$	$^{+1\%}_{-1\%}$
$W^\pm W^\pm jj$ (EW)	NLO in QCD	Eq. (4.2) + diagram removal	254	$^{+1\%}_{-1\%}$	$^{+1\%}_{-1\%}$
Inclusive $W^\pm V$ $(3\ell\nu)$	FxFx (1j)	Eqs. (4.3), (4.4)	2,520	$^{+5\%}_{-6\%}$	$^{+1\%}_{-1\%}$

TABLE IV. Visible signal cross sections (and efficiencies) after applying different selections to the simulated events.

m_N	$\sigma^{\text{Gen.}}$ [fb]	$\sigma^{\text{Pre.}}$ [fb]	($\mathcal{A}$)	σ^{SR} [fb]	(ε)
150 GeV	13.3	3.7	(28%)	0.5	(14%)
1.5 TeV	8.45	3.18	(38%)	1.9	(63%)
5 TeV	1.52	0.58	(38%)	0.46	(79%)
15 TeV	0.190	0.072	(38%)	0.056	(78%)

TABLE V. Expected number of SM background events in the Signal Region at the (HL-)LHC with $\mathcal{L} = 300$ fb^{-1} (3 ab^{-1}).

Collider	QCD $W^\pm W^\pm jj$	EW $W^\pm W^\pm jj$	$W^\pm V(3\ell\nu)$	Total
LHC	0.05	0.52	0.14	0.71
HL-LHC	0.49	5.17	1.40	7.10

Kinematics at NLO+PS

after basis pre-selection

Top: $p_T^{\mu_1}$, $p_T^{\mu_2}$, Btm: $\Delta\varphi(\mu_1,\mu_2)$, MET

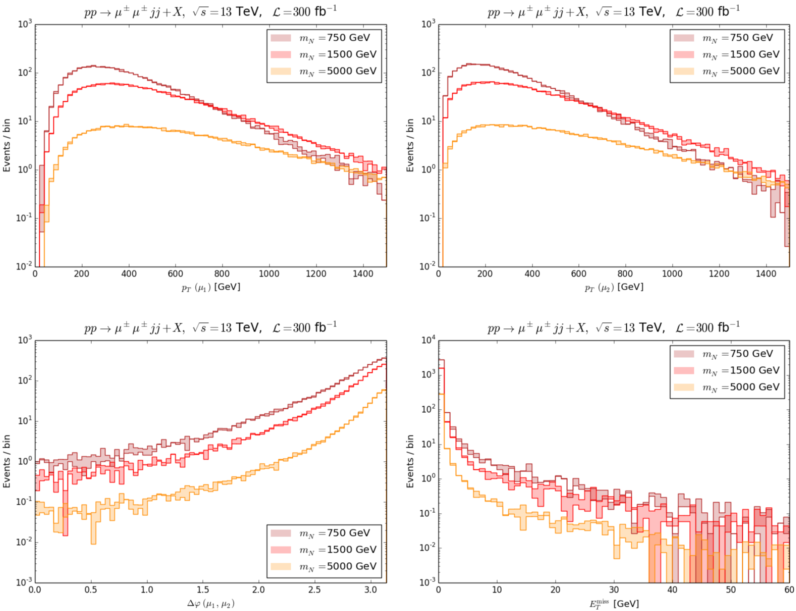

Top: $p_T^{j_1}$, $p_T^{j_2}$, Btm: η^{j_1}, $\Delta\eta(j_1, j_2)$

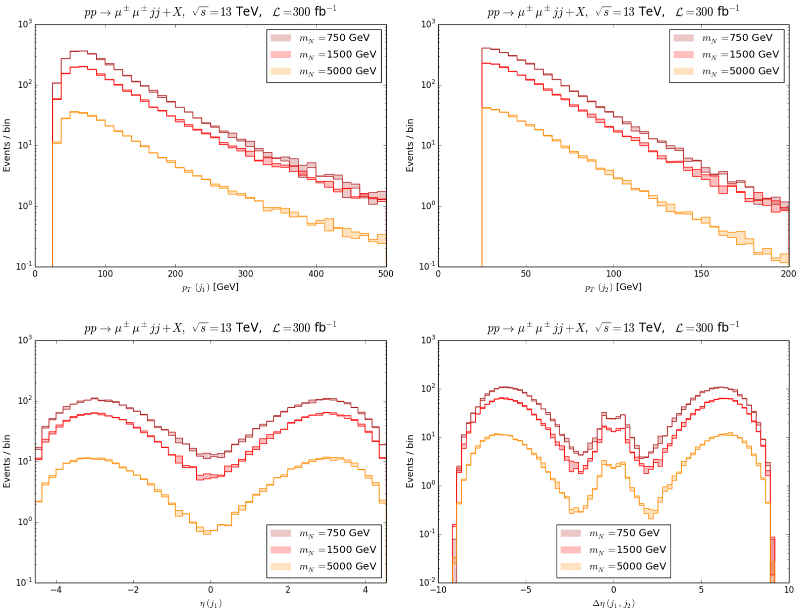

Top: $H_T = \sum |p_T^j|$, $X_T = H_T + \sum |p_T^\mu|$, **Btm:** $H_T/p_T^{\mu_1}$, $X_T/p_T^{\mu_1}$